

FAST CONTINUOUS SWIMMING OF TWO PELAGIC PREDATORS, SAITHE (*POLLACHIUS VIRENS*) AND MACKEREL (*SCOMBER SCOMBRUS*): A KINEMATIC ANALYSIS

By J. J. VIDELER AND F. HESS

Department of Zoology, State University Groningen, P.O. Box 14, 9750 AA Haren, The Netherlands

Accepted 7 October 1983

SUMMARY

Straight, forward, unrestrained swimming behaviour, with periodic lateral oscillations of body and tailfin, was described and compared for saithe and mackerel. A method was developed for kinematic analysis of forward motion, lateral displacements and body curvature, based on a Fourier-series approach.

The dimensionless kinematic quantities showed relatively small variations over large ranges of swimming speeds. The speed range of mackerel was twice as fast as that of saithe. The main difference in swimming style between the species was a somewhat greater tail amplitude and a correspondingly stronger curvature near the caudal peduncle in mackerel than in saithe.

The swimming style of both species yields a Froude efficiency close to the maximum value possible, given the observed amplitude increase in the posterior part.

INTRODUCTION

Pelagic marine fishes, particularly piscivorous predators, are highly adapted to fast continuous swimming. We have chosen two such species belonging to different families to study their kinematics during unrestrained swimming in still water. The mackerel (*Scomber scombrus*, fam. Scombridae) and the saithe (*Pollachius virens*, fam. Gadidae) are both known to be voracious predators exploiting similar prey populations. Both species are of course capable of all kinds of swimming manoeuvres, but we restricted this study to straight, forward swimming with periodic lateral oscillations of body and tail. We present a new way to analyse such swimming motions, resulting in detailed kinematic descriptions. These are used to compare the swimming behaviour of saithe and mackerel, and they will serve as a basis for the dynamic analysis presented in a subsequent paper (Hess & Videler, 1984).

Outlines of top and side views of ciné pictures of these fishes are shown in Fig. 1 and illustrate the streamlined nature of the body in both species. During steady swimming the pectoral and pelvic fins are pressed against the body and the anterior

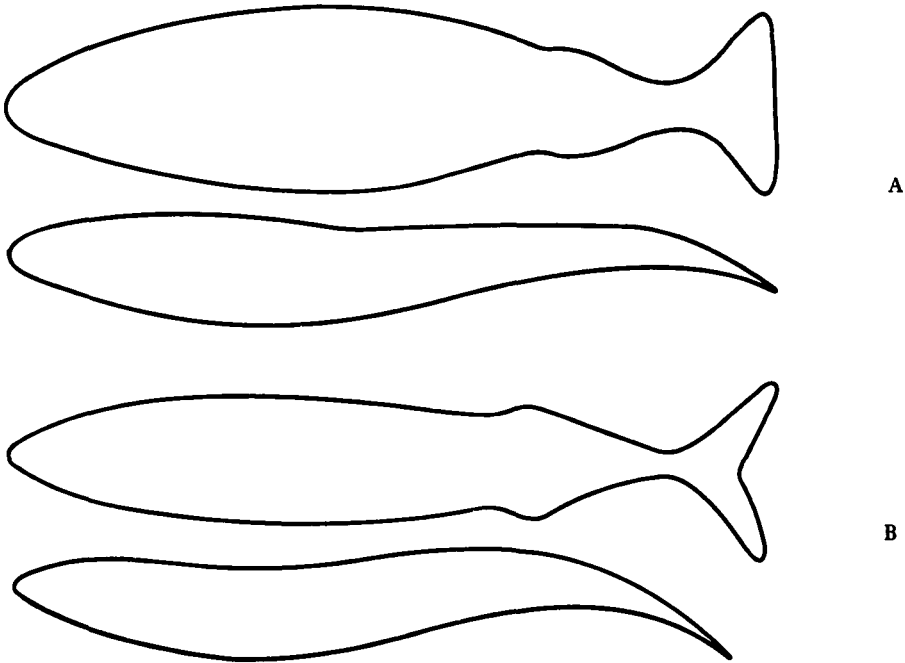


Fig. 1. Top and side views of swimming saithe (A) and mackerel (B), drawn from ciné film images.

parts of dorsal and anal fins are collapsed. The first dorsal fin of the mackerel fits in a groove in the back. The side views show how the last dorsal and anal fins are partly erected and affect the shape of the fish during swimming. The similarity between the pairs of pictures is striking but the tail blades have a different shape and the caudal peduncle of saithe is higher.

Gray (1933), using successive ciné pictures of top views of swimming fish, showed that 'waves of curvature pass along the body from head to tail', and that every point on the body follows a wave track in space in the swimming direction at an average speed lower than the speed of the body wave. A precise description of these wave phenomena for swimming cod was given by Videler & Wardle (1978) and Wardle & Videler (1980a). The use of high-speed ciné film, digitizer, computer and numerical techniques allows us to carry out a more detailed kinematic analysis for saithe and mackerel.

For the comparison of swimming motions of fishes of different sizes and swimming at different speeds it is very convenient to use dimensionless quantities. We therefore shall use the fish length L as a unit of length and the period T as a unit of time. The unit of velocity then becomes L/T .

METHODS

High speed films of saithe and mackerel

Saithe were trained to swim back and forth between feeding points situated at the ends of a 14 m long tank at the DAF's Marine Laboratory in Aberdeen. Films of top views of passing fish were taken with a high-speed camera mounted on a scaffolding

power over the middle of the tank. At that point the tank was 1.2 m wide and 0.8 m deep. In our analysis we use film sequences of one specimen which was 0.35 cm long at first and had grown to 0.40 cm when it was recorded again a few months later.

Swimming mackerel were filmed in a 5 m long tank (1 m wide and 0.8 m deep) at a field station of the Marine Laboratory near Loch Ewe in North West Scotland. Mackerel were caught near the station using lines fitted with unbarbed hooks. Fish were transported in seawater-filled containers and released in the tank within a few minutes after capture. Great care was taken not to touch the animals. Mackerel always started to swim very fast and vigorously immediately after release. The inside of the swimming tank was lined with a plastic sheet, a few centimetres away from the wall, to avoid fatal damage from head-on collisions against the wall. After a few hours they usually relaxed and cruised the tank continuously at more moderate speeds. Film sequences of both types of swimming behaviour of four specimens are used in this paper. A background illumination technique made it possible to film both species at 100 or 200 frames per second without disturbing the behaviour of the fish with high light levels. Details are given elsewhere (Videler, 1981).

We selected only those film sequences which showed regular periodic swimming motions, to a good approximation along a straight horizontal path. We excluded the burst and coast swimming style, frequently used by saithe (Videler & Weihs, 1982) and sometimes by mackerel. Sequences of slow swimming at velocities lower than $1.5 \text{ lengths s}^{-1}$ for saithe and 3 lengths s^{-1} for mackerel were discarded, because the fish swam with extended pectoral fins [see also Gray's (1933) example of a mackerel swimming at $1.2 \text{ lengths s}^{-1}$].

In each sequence the head of the fish entered the field of view of the camera after the camera had reached its set speed of frame rate. The fish subsequently crossed the field of view and the sequence ended when the tail tip disappeared. The camera was fitted with a reference grid, visible on each frame, which was the earth bound frame of reference because the camera was mounted in a fixed position.

The length of the crossing fish was used to scale the pictures. We used the digitized outlines of whole fish images for the analysis of propulsive wave characteristics.

Swimming motion analysis

The circumference of the image of the fish on each frame and two selected points of the reference grid were digitized with an HP 9874A digitizer and an HP 9835A computer. In the tail region the outlines of the fin rays of the middle of the fin were used even if the tailblade was dorsoventrally cambered. The coordinates of the tip of the head and the reference points served to calculate the mean path of motion with standard linear regression equations. This mean path of motion was designed to be the x-axis in a new frame of reference and all coordinates were transformed accordingly. The z-axis was perpendicular to the x-axis and horizontal. For each of the body circumferences a central line dividing the fish image into two lateral halves was computed. On the left and right outline 100 equidistant points were calculated. Point number 1 on both outlines was the tip of the head and the first point on the centre line. Similarly point number 100 was the tailtip and the last point on the centre line. The other points on the centre line were situated half way between equivalent points of the outlines. The centre lines were divided into 99 line segments. The sum of the 99 pieces

was the length of the fish which was supposed to be the same for all the images of one sequence and equal to the average centre line length. Small deviations ($< \pm 2\%$) from the average centre line length, mainly due to digitizing inaccuracies, were eliminated by length corrections. Fig. 2 shows the digitized outlines and computed centre lines for one sequence of saithe. The centre lines were used for the kinematic analysis of the swimming motion. This analysis deals with: the time period, the forward motion, the lateral displacement and the body curvature.

Time period

For the determination of the time period we used two methods. The first method is rather simple. The lateral (z) position of each body point oscillates in time. The time intervals between successive extreme lateral positions are estimates for half of the time period T . The resulting values for T are averaged, after giving each one a weight proportional to the corresponding amplitude. This method can only be applied to body points whose amplitude is greater than the noise present in the digitized data. If the film contains less than one period this method may be rather awkward. The second method is more sophisticated and takes considerably more computing time. For each body point ($p = 1, \dots, 100$) the lateral position $h_p(t)$ as a function of time is approximated by a function of the form:

$$f(t) = a_0 + b_0 t - a_1 \cos \frac{2\pi t}{T} + b_1 \sin \frac{2\pi t}{T}. \quad (1)$$

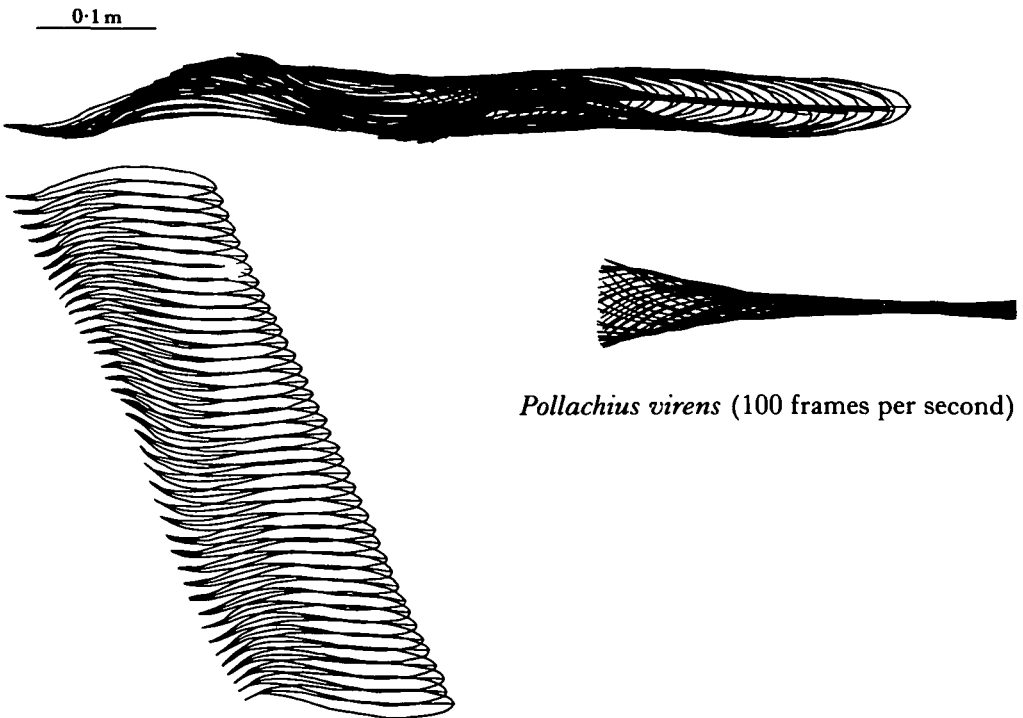


Fig. 2. Digitized film images of a saithe sequence (S1). Top: superimposed circumferences with computed centre lines. Left: the same images at half size shifted laterally for greater clarity. Right: centre lines only, with x -positions of nose made to coincide.

The first two terms represent a straight-line motion and the last two terms a harmonic motion. If the film frames represent the time points t_i , $i = 1, \dots, n$, then a_0 , b_0 , a_1 , b_1 and T must be chosen such that

$$D_p = \sum_{i=1}^n \{h_p(t_i) - f(t_i)\}^2 \quad (2)$$

is minimized. For a chosen fixed value of T , D_p is minimized as a function of a_0 , a_1 , b_0 , b_1 . This is done by solving a 4×4 matrix equation. The resulting value for D_p is a function of T only: $D_p(T)$. This function is minimized by a unidirectional search method (Himmelblau, 1972). For each body point p , we obtain the corresponding optimum value for T : T_p . For any T close enough to T_p , D_p is a quadratic function of T :

$$D_p = A_p + B_p(T - T_p)^2. \quad (3)$$

The final ('best') estimate for T is found by minimizing:

$$\sum_{p=1}^{100} D_p,$$

which is the same as averaging the T_p values with suitable weights. In cases where we used both methods the results were never significantly different. The time period T will be used as a unit of time.

Forward motion

The forward motion of the fish is approximated by a straight-line motion with a constant acceleration or deceleration plus a speed fluctuation originating from the tail beat. We have used the mean distance in the x -direction between nose and tail, L , as a unit of length. (This is about 1 or 2% smaller than the length of the fish when it is straight.) The x -length, L , is approximated by a function of the form:

$$f(t) = a_0 + a_2 \cos 2\omega t + b_2 \sin 2\omega t, \quad \omega = 2\pi/T. \quad (4)$$

A least-squares fit yields the mean value $L = a_0$. The two last terms represent a periodic x -length fluctuation with period $T/2$.

For the forward speed of the fish we take the speed of body point number 25, as this is close to the fish's centre of mass, but this choice is not at all critical. This point's x -position is approximated by a function of the form:

$$f(t) = a_0 + b_0(t - t_c) + c_0(t - t_c)^2 + a_2 \cos 2\omega t + b_2 \sin 2\omega t, \quad \omega = 2\pi/T, \quad (5)$$

where t_c is the time point half way between the first and the last frame. The first three terms represent a motion with constant acceleration, and the other two terms a periodic fluctuation. A least-squares fit yields the following quantities. The mean forward velocity is b_0 , or dimensionless in lengths/period:

$$U = b_0 \cdot T/L. \quad (6)$$

The mean acceleration is $2c_0$, or dimensionless in lengths/period²:

$$\dot{U} = 2c_0 \cdot T^2/L \quad (7)$$

and the amplitude of the periodic velocity fluctuation in lengths/period:

$$\Delta U = 4\pi(a_2^2 + b_2^2)^{1/2}/L. \quad (8)$$

The observed speed fluctuations turn out to be insignificant. As for the acceleration, it is not so much \dot{U} , but rather the quantity $\beta = \dot{U}/U^2$ which is of hydrodynamic relevance (Hess & Videler, 1984). β is the relative velocity increase during the time it takes to move one fish length; we call it the acceleration parameter.

Lateral displacement

The bulk of the kinematic analysis concerns the lateral motion of the fish body. In this analysis we assume that the forward motion of all body points is uniform. This implies that in the coordinate system which moves with the fish at speed U , the body points move in a lateral (z) direction only. The x -component of the motion is ignored. This assumption is justified as long as the amplitudes of all body points are small enough. In reality the situation may be somewhat different, but the differences are never so large as to influence our conclusions. The fish stays close to the x -axis and occupies a region between $x = 0$ (nose) and $x = L$ (tail) (see Fig. 3). In terms of L , the nose is at $x = 0$ and the tail at $x = 1$. The centre line of the fish is described by the equation:

$$z = h(x, t). \quad (9)$$

The digitized data contain values for $h(x, t)$ at 100 body points, $x_p = (p-1)/99$ ($p = 1, \dots, 100$) and at certain time points, t_i ($i = 1, \dots, n$). These values contain errors. We want to obtain a smooth function $h(x, t)$ which closely fits the data. First we consider $h(x, t)$ as a function of time. Since it is periodic with period T , it can be represented by a Fourier series. We make a least-squares approximation as indicated by:

$$h(x, t) \approx a_0(x) + b_0(x) (t - t_c) + \sum_{j=1}^5 [a_j(x)\cos j\omega t + b_j(x)\sin j\omega t]. \quad (10)$$

The first two terms represent a straight-line motion. Frequencies higher than the fifth need not be included as their contributions drown in the noise. Ideally, for each

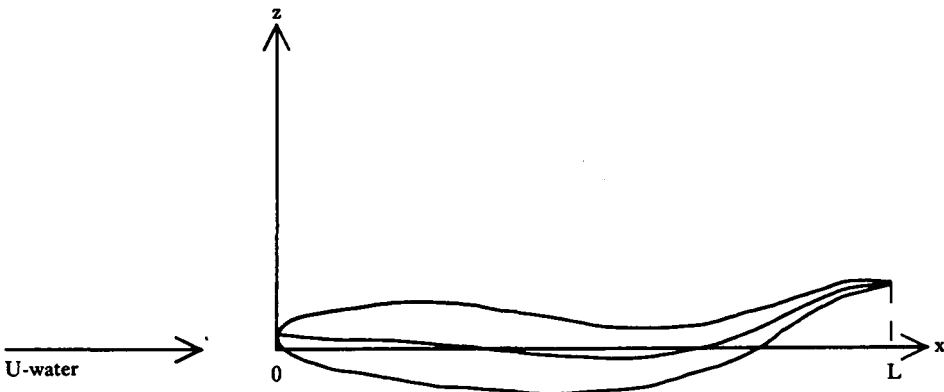


Fig. 3. Coordinate system x, z . The water moves with velocity U in the x -direction.

point x_p we should obtain the same a_0 , and b_0 should vanish. Moreover, because of lateral symmetry we have:

$$h(x,t) - a_0 = -[h(x,t + T/2) - a_0]$$

and all Fourier terms with even frequencies should vanish. After the fit, we only retain the odd Fourier terms, which constitute an idealized motion distilled from the recorded motion. This procedure is justified if the rejected terms are small. In the 13 film sequences of saithe the a_0 values never differed by more than $0.02L$, and $|b_0| \leq 0.04L/T$. The ratio between second frequency amplitude and first frequency amplitude, a_2/a_1 , in the tail region is ≤ 0.03 in half of the cases, and in the worst case (S9) it reaches ~ 0.15 . The path curvature as seen from above is strongest for one mackerel sequence (M8): $L/R \approx 0.06$, where R is the path's radius. In all other selected cases it is much weaker. Thus the following approximation for $h(x,t)$ appears to be reasonably accurate in most of the 25 selected cases:

$$h(x,t) \approx \sum_{j=1,3,5} \{a_j(x)\cos j\omega t + b_j(x)\sin j\omega t\}. \quad (11)$$

For each body point we now have six Fourier coefficients, a_j and b_j , characterizing the lateral motion of the fish body. Now we consider $h(x,t)$ as a function of x . We obtain a smooth function in x by the use of cubic splines (Ahlberg, Nilson & Walsh, 1967). For each of the six Fourier coefficients a least-squares approximation in terms of cubic splines is made. The fish's centre line is divided into 20 segments by 21 equidistant points (so-called knots) including nose and tail. On each of the segments a cubic spline is a third degree polynomial. The spline and its first and second derivatives are continuous across the division points (knots). At the nose and tail points we must impose end conditions. We choose the condition of vanishing curvature: the second derivative with respect to x must vanish: $h''(x,t) = 0$ at $x = 0$ and at $x = 1$. This is reasonable for the nose, but what about the tail? The motion picture images indeed show that the fish tail is far less curved at the end than near the caudal peduncle. As a check we made an approximation with alternative end conditions: curvature at end point equals curvature at next knot. This led to almost identical results. A spline is completely determined by its values at the knots. After the fit we obtain for each Fourier component 21 numbers representing the values of the coefficient at the knots $x_k = (k-1)/20$, $k = 1, \dots, 21$. Thus the lateral motion of the fish is described by a smooth function $h(x,t)$ which is characterized by 6×21 numbers.

The smoothing of the lateral motion, first in time by a sum of Fourier terms, then along the body by cubic splines, retains all the significant features and removes much of the noise from the data. As regards the time dependence, since we include Fourier terms up to the fifth frequency, differences in $h(x,t)$ for time points separated by intervals down to about $T/20$ can be taken into account. It turns out that the first frequency accounts for most of the lateral motion, the third frequency contributes something in the posterior part of the fish and the fifth frequency contributions can hardly be distinguished from noise. In the smoothing by splines we used 20 segments along the body, therefore differences in $h(x,t)$ for body points separated by distances down to $L/20$ can be taken into account. This resolution turns out to

be quite sufficient, considering the noise in the data. Taking fewer knots would remove more noise from the Fourier coefficients but might also lead to some loss of information.

The resulting, smoothed function $h(x,t)$ can also be written in the form:

$$h(x,t) = \sum_{j=1,3,5} h_j(x) \cos j\omega[t - \tau_j(x)]. \tag{12}$$

Here $h_j(x)$ is the amplitude at point x belonging to frequency j , and $\tau_j(x)$ is the phase function; it represents the instant at which the contribution of frequency j reaches its maximum at x . Therefore multiples of T/j may be added to $\tau_j(x)$ or subtracted from it. The functions $h_j(x)$ and $\tau_j(x)$ are related to the Fourier coefficients $a_j(x)$ and $b_j(x)$ by:

$$\left. \begin{aligned} a_j(x) &= h_j(x) \cos j\omega\tau_j(x) \\ b_j(x) &= h_j(x) \sin j\omega\tau_j(x) \end{aligned} \right\} \tag{13}$$

$$\left. \begin{aligned} \text{and } h_j(x) &= \{a_j^2(x) + b_j^2(x)\}^{1/2} \\ \tau_j(x) &= \frac{1}{j\omega} \arctan \frac{b_j(x)}{a_j(x)}. \end{aligned} \right\} \tag{14}$$

The functions $h_j(x)$ and $\tau_j(x)$ ($j = 1, 3, 5$) are shown in Fig. 4 for one saithe sequence (S1). The h_j values are expressed in units L , and the τ_j values in units T . In these units $\omega = 2\pi$. The origin of the time scale has been chosen to coincide with the instant of maximum first frequency tail point deflection: $\tau_1(1) = 0$ by definition. This convention is adopted throughout this paper.

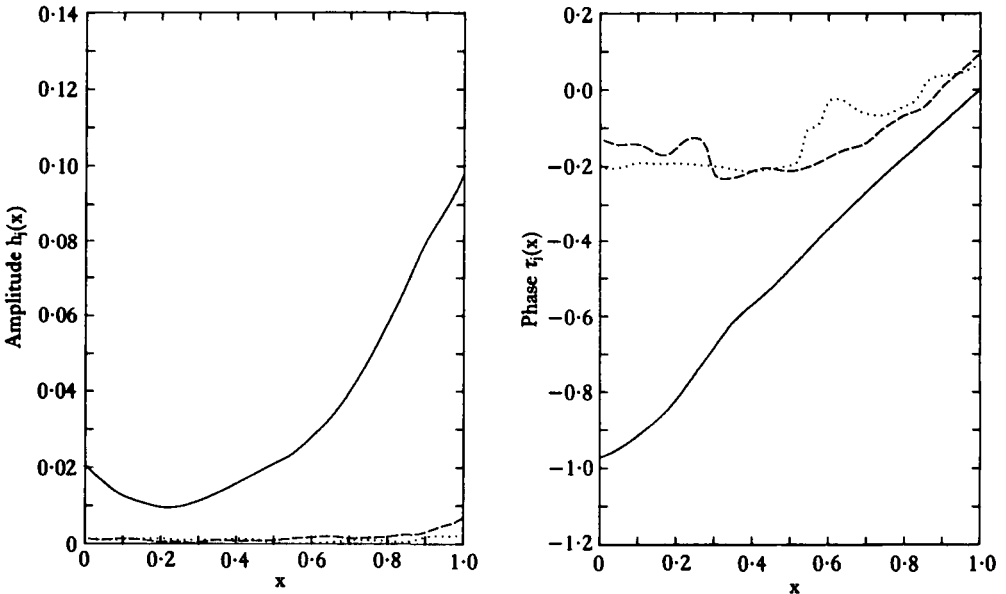


Fig. 4. Lateral deflection $h(x,t)$ for saithe sequence S1. Left: amplitude curves $h_j(x)$. Right: phase curves $\tau_j(x)$. For explanation see text. Drawn curves, first frequency; dashed, third frequency; stippled, fifth frequency contribution.

Obviously, the first frequency contribution is by far the most significant. Clearly a wave of lateral deflection runs along the fish body from nose to tail. The amplitude of this wave is greatest at the tail end, smallest at about one-quarter of the length from the nose, and somewhat less small at the nose point. The speed at which the wave runs along the body can be deduced from the graph for $\tau_1(x)$. The steeper this curve, the slower the wave speed. The body wave length is roughly equal to the fish length. In some previous publications (Videler & Wardle, 1978; Wardle & Videler, 1980a) this running wave is assumed to have a constant speed. Indeed, we can approximate $\tau_1(x)$ by a straight line. We do this by a least-squares fit, giving each body point a weight proportional to the amplitude $h_1(x)$. The resulting estimate for the constant wave speed is called V . V typically is about 1.0 length/period in both saithe and mackerel. The wave speed may considerably deviate from its mean value, especially in the anterior part of the fish (Fig. 4). In the posterior half it appears to be more constant. Since the motion of the tail region is of particular hydrodynamic interest (Lighthill, 1960, 1969) we repeated the above straight-line fit for the posterior half of the fish. Both values for V are listed in Tables 1 and 2.

Fig. 4 shows that the third and fifth frequency contributions are only significant in the posterior part of the fish. Therefore, the phase curves $\tau_3(x)$ and especially $\tau_5(x)$ have little meaning outside the tail region.

Body curvature

The second derivative of $h(x,t)$ with respect to x , $h''(x,t)$, is a measure for the lateral body curvature. In fact, h'' equals $1/r$, where r is the radius of curvature, provided h' is small enough. We name h'' : $f(x,t)$. For this curvature function we have the representation:

$$f(x,t) = \sum_{j=1,3,5} \{a_j''(x)\cos j\omega t + b_j''(x)\sin j\omega t\}. \quad (15)$$

As a_j and b_j are piecewise cubic functions, their second derivatives are piecewise linear and not smooth at the knots. We therefore fit splines to the first derivatives a_j' and b_j' and differentiate those splines ('spline on spline' method, see Ahlberg *et al.* 1967) rather than differentiating the original splines twice. This results in a reasonably smooth curvature function $f(x,t)$ which can also be written in the form

$$f(x,t) = \sum_{j=1,3,5} f_j(x)\cos j\omega[t - \sigma_j(x)]. \quad (16)$$

Here the $f_j(x)$ values are the curvature amplitude functions, and $\sigma_j(x)$ values are the curvature phase functions. These are shown in Fig. 5, again for the same sequence (S1). Generally, when a part of the fish body is deflected to the right, the left side is concave and *vice versa*. Hence, for any body point the curvature and lateral position nearly always have opposite signs. Therefore, the curvature plots are made for $-f(x,t)$ rather than for $f(x,t)$. It means that the phase curves $\sigma_j(x)$ are shifted up or down by $0.5/j$, which makes it easier to compare the curvature phase curves with the corresponding $\tau_j(x)$ in Fig. 4. For instance, $\sigma_1(x) + 0.5$ does not differ much from $\tau_1(x)$.

Many of the small-scale undulations in these graphs are caused by noise in the original data. But again it is clearly visible that a wave (this time a lateral curvature

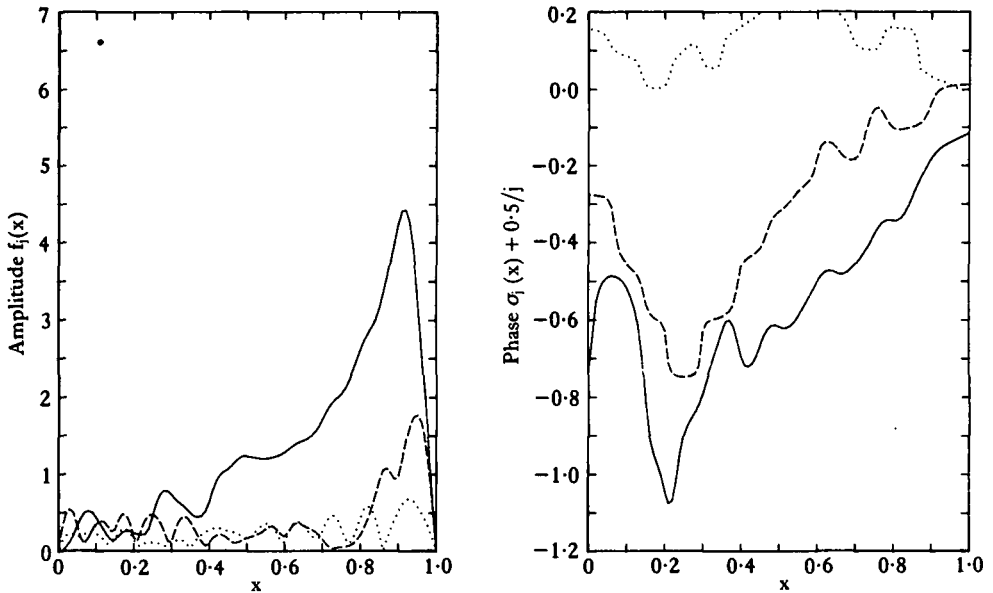


Fig. 5. Body curvature $-f(x,t)$ for saithe sequence S1. Left: amplitude curves. Right: phase curves. For explanation see text. Drawn curves, first frequency; dashed, third frequency; stippled, fifth frequency contribution.

wave) runs from the anterior part of the body to the tail. The amplitude is greatest just behind the caudal peduncle, i.e. in the anterior part of the tail, where it reaches a value of about 4. The radius of curvature r in this region can become as small as $L/4$. The front part of the fish hardly bends at all, and the curvature as drawn in Fig. 5 represents more noise than real bending. Therefore, the phase curves have no physical meaning in the anterior 25% of the length of the fish, and for the higher frequencies probably the anterior 75%.

RESULTS AND DISCUSSION

Kinematic quantities derived from each film sequence are given for saithe in Table 1 and for mackerel in Table 2. The columns of these tables contain, from left to right: the name of the film sequence, the fish specimen, the length of the fish L in metres, the time period T in seconds, the swimming speed u in fish lengths per second, the dimensionless speed U in lengths/period, the acceleration \dot{U} in lengths/period², the acceleration parameter $\beta = \dot{U}/U^2$, the first frequency amplitude at the tailpoint $a = h_1(1)$ in lengths, the body wave speed V in lengths/period as obtained from a straight-line fit over the whole fish body, the ratio U/V , and again V and U/V , but now for the posterior half of the fish only. The bottom line of each table gives values for the 'average' saithe and the 'average' mackerel. The meaning of 'average' will be explained below.

Before discussing the results it is useful to consider the accuracy of these data. The period T has an accuracy of about 1%. For the quantities U , \dot{U} and a we compared

Table 1. *Kinematic data for saithe*

Filmshot	Specimen								Whole body		Posterior half	
		L	T	u	U	\dot{U}	β	a	V	U/V	V	U/V
S1	A	0.35	0.287	3.0	0.86	0.02	0.03	0.098	1.03	0.84	1.09	0.79
S2	A	0.35	0.446	1.8	0.81	-0.00	-0.01	0.067	0.92	0.88	0.98	0.83
S3	A	0.35	0.374	2.1	0.79	0.02	0.04	0.088	1.01	0.78	1.08	0.73
S4	A	0.35	0.305	2.7	0.84	0.04	0.06	0.092	1.05	0.80	1.07	0.78
S5	A	0.35	0.188	3.5	0.67	0.14	0.32	0.101	0.98	0.68	1.06	0.64
S6	A	0.35	0.261	3.1	0.82	0.07	0.10	0.098	1.00	0.82	1.11	0.74
S7	A	0.35	0.272	2.9	0.80	0.05	0.07	0.095	1.02	0.78	1.06	0.76
S8	A	0.35	0.515	2.3	1.21	-0.12	-0.08	0.078	1.16	1.04	1.27	0.95
S9	A	0.40	0.178	5.5	0.99	-0.07	-0.07	0.075	0.98	1.01	1.03	0.96
S10	A	0.40	0.222	3.3	0.75	0.01	0.02	0.091	0.92	0.82	0.97	0.77
S11	A	0.40	0.206	3.4	0.70	0.06	0.11	0.077	0.91	0.77	0.96	0.73
S12	A	0.40	0.150	6.2	0.94	-0.05	-0.05	0.064	0.90	1.04	0.94	1.00
S13	A	0.40	0.215	4.4	0.95	-0.04	-0.04	0.059	0.96	0.99	0.97	0.98
Average			0.278		0.86		0.04	0.083	0.98	0.87	1.04	0.82

L, length of fish (m); T, time period (s); u, swimming speed (fish lengths s⁻¹); U, dimensionless speed (lengths/period); \dot{U} , acceleration (lengths/period²); β , acceleration parameter ($\beta = \dot{U}/U^2$); a, first frequency amplitude at the tailpoint [$a = h_1(1)$]; V, body wave speed (lengths/period).

Table 2. *Kinematic data for mackerel*

Filmshot	Specimen								Whole body		Posterior half	
		L	T	u	U	\dot{U}	β	a	V	U/V	V	U/V
M1	B	0.33	0.206	4.0	0.83	-0.04	-0.05	0.092	1.02	0.81	1.12	0.74
M2	B	0.33	0.196	4.0	0.80	0.00	0.00	0.104	1.01	0.79	1.21	0.66
M3	B	0.33	0.224	3.9	0.88	-0.01	-0.01	0.107	1.22	0.72	1.30	0.68
M4	B	0.33	0.186	5.0	0.93	0.05	0.06	0.108	1.08	0.86	1.18	0.79
M5	C	0.34	0.067	11.2	0.76	0.06	0.10	0.102	0.94	0.81	1.06	0.72
M6	C	0.34	0.072	10.2	0.74	0.04	0.07	0.106	1.00	0.74	1.02	0.73
M7	C	0.34	0.082	9.2	0.76	0.10	0.18	0.107	0.94	0.80	1.06	0.71
M8	D	0.30	0.154	5.3	0.82	-0.02	-0.04	0.083	1.02	0.81	1.30	0.63
M9	D	0.30	0.179	4.5	0.82	0.04	0.06	0.104	1.15	0.71	1.24	0.66
M10	E	0.31	0.083	8.6	0.72	0.13	0.26	0.117	0.95	0.76	1.13	0.64
M11	E	0.31	0.181	4.9	0.90	0.05	0.06	0.112	1.01	0.90	1.19	0.76
M12	E	0.31	0.201	5.1	1.04	0.05	0.04	0.112	1.10	0.95	1.25	0.83
Average			0.153		0.83		0.06	0.104	1.02	0.81	1.16	0.72

L, length of fish (m); T, time period (s); u, swimming speed (fish lengths s⁻¹); U, dimensionless speed (lengths/period); \dot{U} , acceleration (lengths/period²); β , acceleration parameter ($\beta = \dot{U}/U^2$); a, first frequency amplitude at the tailpoint [$a = h_1(1)$]; V, body wave speed (lengths/period).

the listed values with those obtained from the same film sequences by another method: only the nose and tailpoints were digitized and subsequently analysed. The differences between the results of both methods are for U: <0.02, for β : <0.05 and for a: $\leq 5\%$ (except for S8 and M3 where it is $\sim 10\%$).

The most striking trend in the results is that in spite of the large variations in swimming speed (u ranges from 1.8–6.2 lengths s⁻¹ in saithe and from 3.9–11.2 lengths s⁻¹ in mackerel), the dimensionless quantities U, a and V vary relatively little, whereas the swimming speeds, u, vary by a factor of about three for both species. For

saithe U lies between 0.70 and 1.21 (factor 1.7), V (posterior half) between 0.94 and 1.27 (factor 1.4), U/V between 0.64 and 1.00 (factor 1.6), and a between 0.059 and 0.101 (factor 1.7). For mackerel U lies between 0.72 and 1.04 (factor 1.4), V between 1.02 and 1.30 (factor 1.3), U/V between 0.63 and 0.83 (factor 1.3) and a between 0.083 and 0.117 (factor 1.4). In the case of mackerel such variations may be partly due to differences in swimming style between individual specimens. However, it appears that both species have a swimming style which stays roughly the same through a wide range of speeds.

A quantity mentioned before, but not listed in the tables is ΔU , the amplitude of the periodic speed fluctuations. For the saithe film sequences it lies between 1 and 5 % of U . (The 5 % case is S5, which has the greatest acceleration.) But if the phase relationship with the tail position is taken into account, these fluctuations yield an average amplitude of only 0.6 % of U for the 13 cases, which is negligible. Considering the estimated accuracy of our results, we conclude that the periodic speed fluctuations, in as far as they are correlated with tailbeat, are smaller than 2 % for saithe. For mackerel we did not actually calculate the average, but the situation appears to be the same.

Comparison of swimming styles

In the analysed sequences the lowest and highest swimming speeds of mackerel are about twice as high as those of saithe. Data from the literature indicate that the speed ranges presented here give a good impression of the capabilities of the two species. Our maximum velocity for saithe of 6.2 lengths s^{-1} is very close to the maximum burst swimming speed of 6.4 lengths s^{-1} recorded by Blaxter & Dickson (1959). We observed steady swimming without the use of pectoral fins at velocities higher than 1.5 lengths s^{-1} , which is half the maximum sustained cruising speed of saithe found by Greer Walker & Pull (1973). Wardle (1979) recorded a minimum muscle contraction time for a 0.35-m mackerel of about 0.03 s, which would give $T = 0.06$ s, corresponding to our fastest mackerel in sequence M5 (see also Wardle & Videler, 1980b).

Let us now consider more closely the similarities and differences between the analysed cases. For both saithe and mackerel u appears to be proportional to $1/T$ (which implies that U does not vary much) (Fig. 6A). Such a linear relationship was first found by Bainbridge (1958). Indeed, we would theoretically expect (ignoring viscous effects) that a fish can maintain exactly the same swimming style at all swimming speeds, in other words, that the dimensionless quantities remain the same, all velocities (in the fish body as well as in the water) scaling up or down with the tailbeat frequency.

The variations showing up in Tables 1 and 2 may be partially due to differences in acceleration. Fig. 6 (B, C, D) contains plots for U , U/V and a against the acceleration parameter β . We see that for both saithe and mackerel there is a trend of U decreasing with increasing β , as expected. A similar trend is found for U/V , but only with saithe. The tail amplitude (a) increases with β for both species; a seems to be more strongly correlated with acceleration (β) than with actual swimming speed u , as indicated by Fig. 6E. For both saithe and mackerel, the wave speed V (posterior half) shows a positive correlation with the period T (Fig. 6F). Regression lines have not been drawn in the graphs, but we list them here with the correlation coefficients between brackets. (T is in seconds, u in lengths s^{-1} and the other quantities are dimensionless.)

Saithe	Mackerel
$u = -0.03 + 0.85^{1/T} (+0.91)$	$u = 1.08 + 0.66^{1/T} (+0.99)$
$U = 0.90 - 1.01\beta (-0.76)$	$U = 0.86 - 0.44\beta (-0.42)$
$U/V = 0.86 - 0.94\beta (-0.86)$	$U/V = 0.72 - 0.06\beta (-0.09)$
$a = 0.080 + 0.086\beta (+0.64)$	$a = 0.100 + 0.068\beta (+0.65)$
$a = 0.099 - 0.0047u (-0.43)$	$a = 0.100 + 0.0067u (+0.19)$
$V = 0.90 + 0.54T (+0.66)$	$V = 0.99 + 1.21T (+0.76)$

These regression lines should be considered with caution, as the scatter in the data is relatively large.

From Tables 1 and 2 and also from Fig. 6 it is obvious that there is an overlap between the data for saithe and for mackerel. This is clearly visible in Fig. 7, in which the first frequency lateral displacement functions $h_1(x)$ and $\tau_1(x)$ are drawn for four cases: S1, S3, M2 and M12. The differences between saithe and mackerel do not appear to be significantly greater than the differences between sequences of the same species. What then is the difference in swimming style between saithe and mackerel?

To answer this question we constructed an 'average' saithe and an 'average' mackerel as follows. For each species separately the smoothed lateral displacement functions $h(x,t)$ from all sequences were averaged. Before averaging, the point $t = 0$ was made to coincide with the instant of maximum first frequency tail point deflection as mentioned before. Since a part of the variation in $h(x,t)$ between the sequences is due to errors in the data, the averaged $h(x,t)$ is smoother. In particular the noise in the third and fifth frequency contributions is much reduced. The results for both saithe and mackerel are shown in Fig. 8 for the lateral displacement and in Fig. 9 for the curvature function $-f(x,t)$. The bottom lines in Tables 1 and 2 list the values found for a and V . The values for T , U and β are obtained by averaging the values of the individual cases. From this follows U/V .

Figs 8 and 9 show very clearly that there is a remarkable similarity between the swimming of saithe and mackerel. The tail amplitude is somewhat greater in mackerel, and the curvature near the caudal peduncle is correspondingly stronger in mackerel than in saithe. Otherwise the lateral bending in both fish appears to be the same. The difference in the average acceleration parameter β is far too small to explain the difference in amplitude a . As noted before, the 'average' mackerel swims almost twice as fast as the 'average' saithe. This is the most obvious difference between the species.

It appears that saithe and mackerel have nearly the same swimming style. The main differences found concern the tail amplitude, which is about 25 % greater in mackerel than in saithe, and the wave speed V in the posterior half of the body, which in mackerel is about 10 % greater than in saithe. As in both species U varies around an average value of roughly 0.85, the ratio U/V is smaller on average in mackerel (0.72) than in saithe (0.82).

In nearly all film sequences for both saithe and mackerel, the third frequency contribution at the tail reaches its maximum just after the first frequency contribution does, the phase difference typically amounting to slightly less than $0.1T$. This deviation

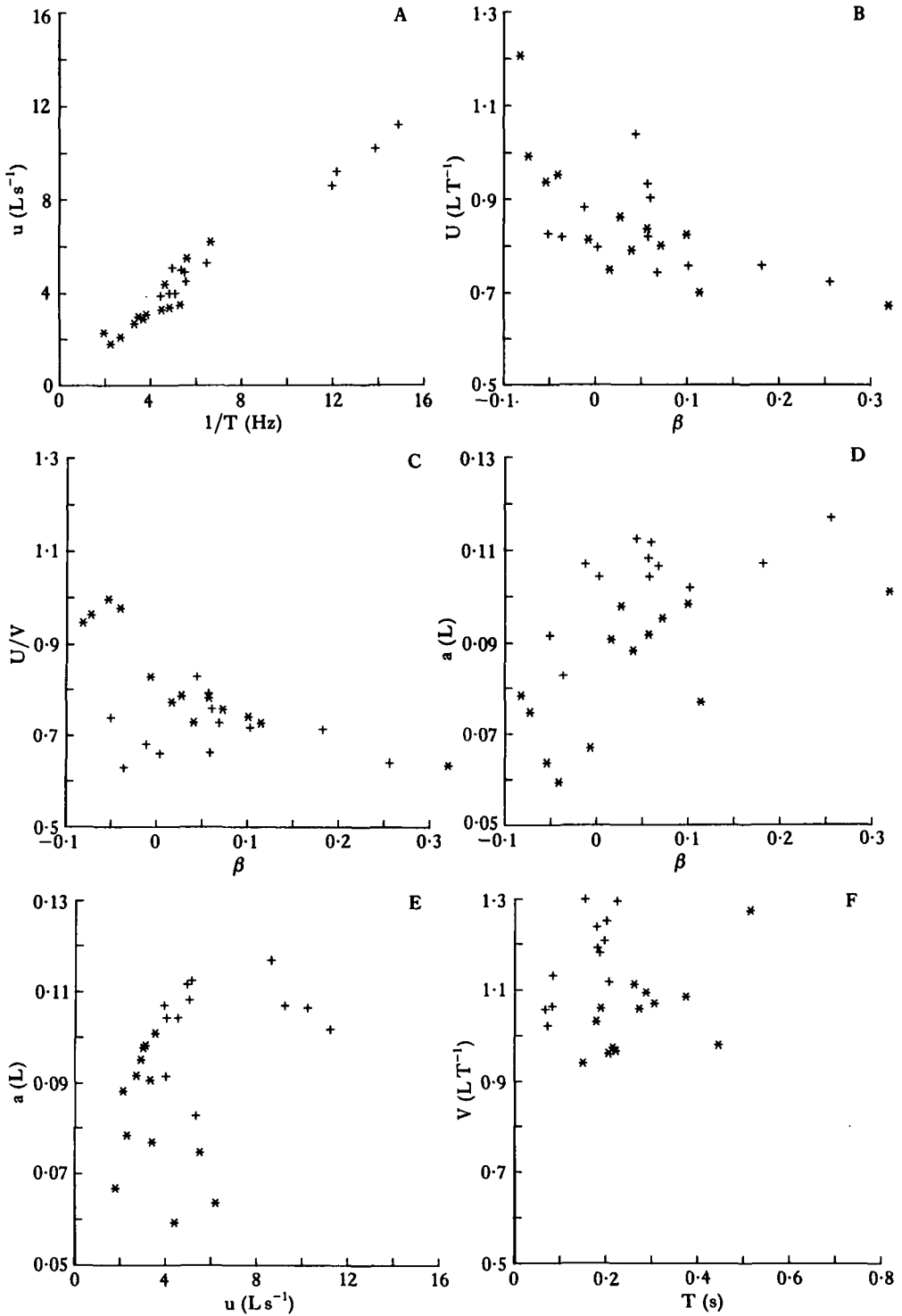


Fig. 6. Some kinematic data for saithe (*) and mackerel (+). (A) Swimming speed u ($L s^{-1}$) vs tailbeat frequency $1/T$ (s^{-1}). (B) Dimensionless swimming speed U ($L T^{-1}$) vs acceleration parameter β . (C) U/V (posterior half) vs β . (D) First frequency tailpoint amplitude a (L) vs β . (E) a (L) vs u ($L s^{-1}$). (F) Body wave speed (posterior half) V ($L T^{-1}$) vs period T (s).

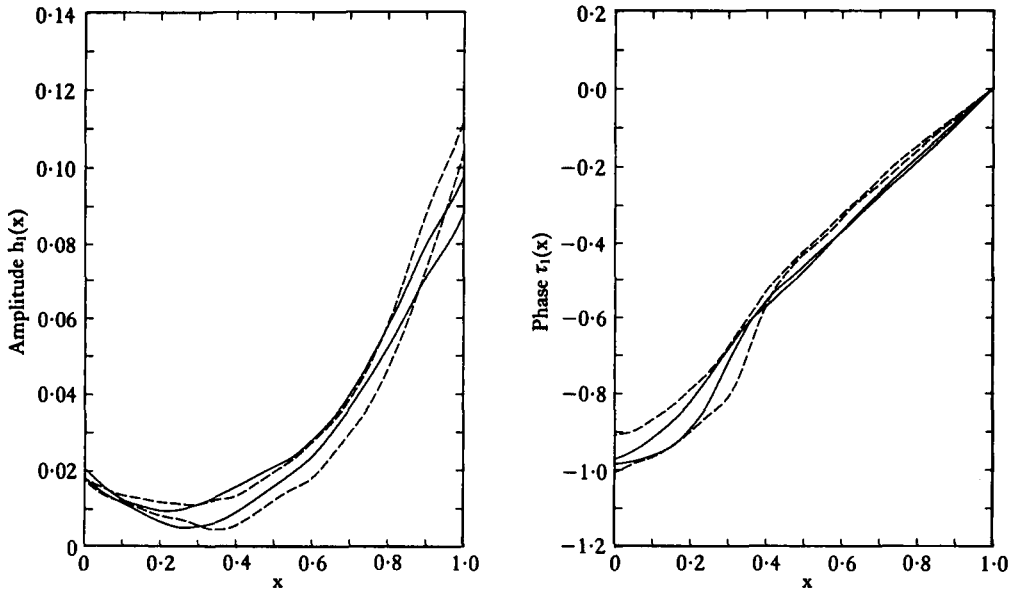


Fig. 7. Lateral displacement (first frequency contribution only) for two saithe and two mackerel, taken as representative examples. Left: amplitude functions $h_1(x)$. Right: phase functions $\tau_1(x)$. For explanation see text. Drawn curves are for saithe (S1, S2), dashed curves for mackerel.

from a pure sinusoidal motion is more easily seen in Fig. 10. Here, for 11 equidistant points on the body of 'average' saithe (Fig. 10A) and mackerel (Fig. 10B), the lateral deflection $h(x,t)$ is plotted as a function of time during one period. In addition, the lateral velocity $\delta h/\delta t$ is shown. The tailpoints reach their maximum velocity just before they cross the plane $z=0$. The third quantity plotted is the local angle of incidence $\alpha(x,t)$, which is the angle between the fish's centre line and the local direction of motion. It is derived from $h(x,t)$ as follows:

$$\left. \begin{aligned} \delta h/\delta x &= \tan\theta \\ \delta h/\delta t &= U \tan\psi \\ \alpha &= -(\theta + \psi). \end{aligned} \right\} (17)$$

The angle θ between centre line and the x -axis does not exceed $\pm 30^\circ$.

Efficiency

Although this paper deals with kinematics rather than dynamics, it seems appropriate at this point to make a simple estimate for the hydrodynamic efficiency. We use formula (8) from Lighthill's (1960) paper on small-amplitude slender-body theory as a starting point. The Froude efficiency is the ratio between the useful work and the total mechanical work done by the fish, the useful work being the total work minus the kinetic energy imparted to the water. Let us ignore the higher frequency contributions, and let V be the body wave speed in the tail region: $\tau_1(x) = (x-1)/V$. Then we have for the function $h(x,t)$ in the tail region:

$$h(x,t) = h_1(x) \cos 2\pi \left(t - \frac{x-1}{V} \right). \quad (18)$$

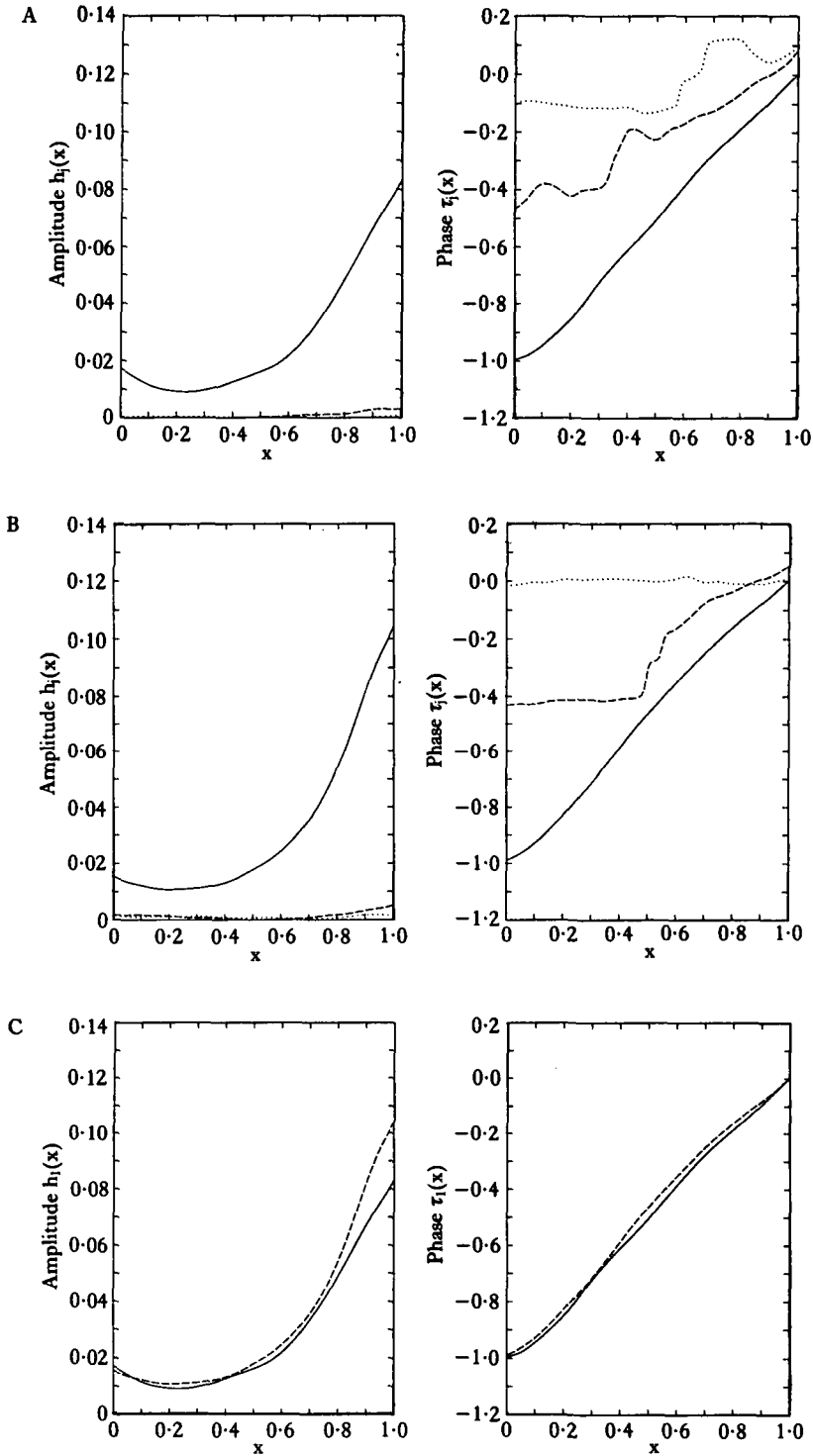


Fig. 8. Lateral displacement $h(x,t)$ for 'average' saithe and 'average' mackerel. (A) Amplitude and phase functions for 'average' saithe. Drawn curves, first frequency; dashed, third frequency; stippled, fifth frequency contribution. (B) The same for 'average' mackerel. (C) Comparison between 'average' saithe (drawn) and 'average' mackerel (dashed), for first frequency only.

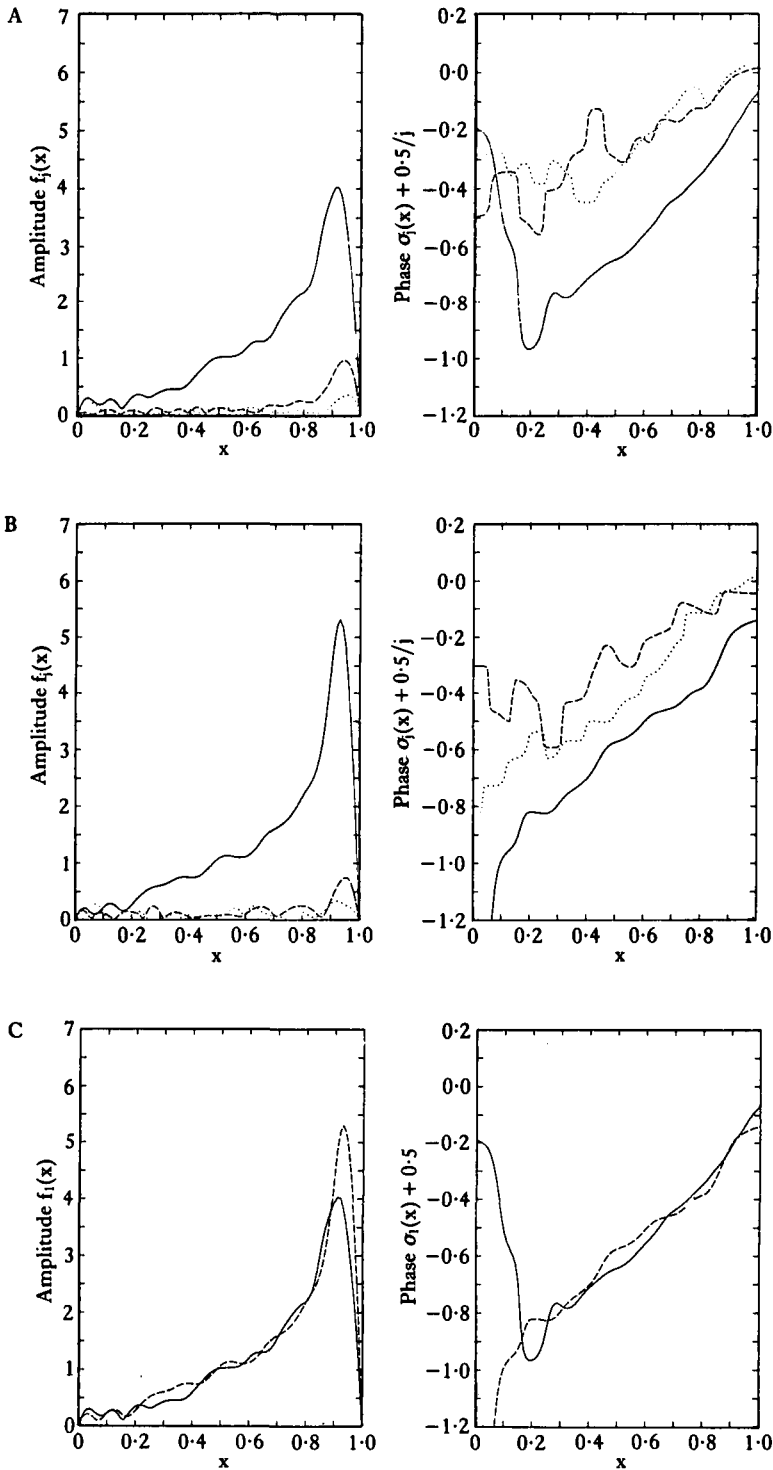


Fig. 9. Body curvature $-f(x,t)$ for 'average' saithe and 'average' mackerel. (A) Amplitude and phase functions for 'average' saithe. Drawn curves, first frequency; dashed, third frequency; stippled, fifth frequency contribution. (B) The same for 'average' mackerel. (C) Comparison between 'average' saithe (drawn) and 'average' mackerel (dashed), for first frequency only.

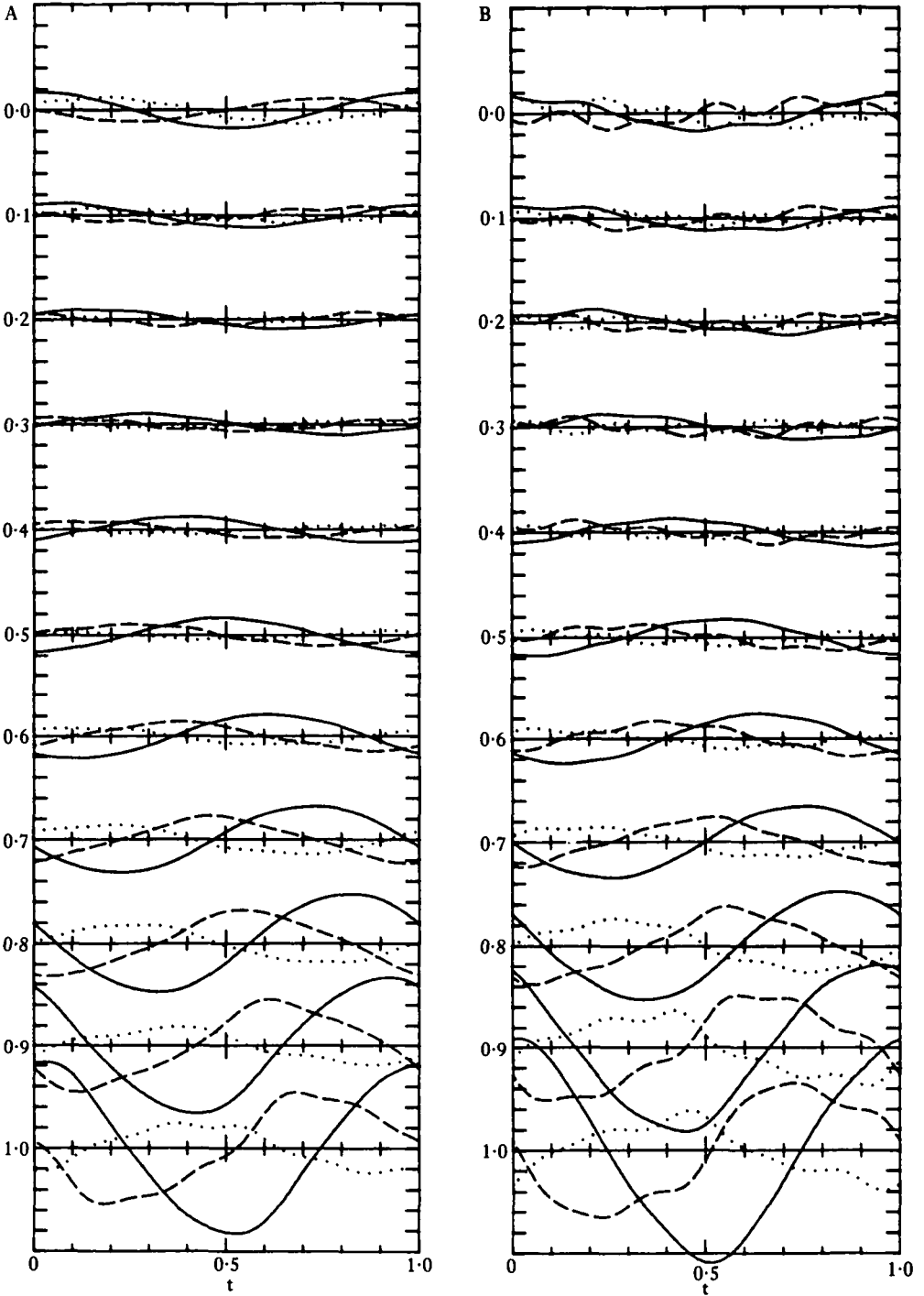


Fig. 10. Lateral deflection h , lateral velocity $\delta h / \delta t$ and local angle of incidence α (see text) for 'average' saithe (A) and 'average' mackerel (B), at 11 equidistant points including nose and tail points. Numbers at left indicate position along body (in units L) from nose. Vertical subdivisions: $0.02 L$ for h (drawn curves); $0.2 L T^{-1}$ for $\delta h / \delta t$ (dashed curves) and 0.2 radians ($= 11.5^\circ$) for α (stippled curves).

For this lateral motion the Froude efficiency is found to be [see Lighthill, 1960, formulae (13) and (14)]:

$$\eta = 1/2(1 + U/V) - 1/2 \frac{q^2}{1 - U/V} \quad (19)$$

where

$$q = \frac{Uh_1'(1)}{2\pi h_1(1)}.$$

If the amplitude $h_1(x)$ is constant near $x = 1$, then q vanishes and only the first term in (19) is left. [In several articles on the swimming of fish (e.g. Webb, 1975; Videler & Wardle, 1978) this term is used as an expression for the 'propeller efficiency'.]

For fixed q , η reaches its maximum value, $1 - |q|$, if $U/V = 1 - |q|$. According to Fig. 8 we have for both saithe and mackerel: $h'(1)/h(1) \approx 2$, and $U \approx 0.8$, hence $q \approx 0.25$. Under these conditions the maximum Froude efficiency is $\eta \approx 0.75$ for $U/V \approx 0.75$, and $\eta > 0.70$ as long as U/V lies between 0.54 and 0.86.

All mackerel sequences have U/V values within this range, and only in four cases of decelerating saithe is U/V outside this range (nearly 1.0). It appears therefore that, given the observed amplitude increase in the posterior part, the swimming style of saithe and mackerel yields a Froude efficiency which is close to the maximum possible value.

A Royal Society Fellowship to JJV made collection of the filmed data possible in close stimulating cooperation with Dr C. S. Wardle (Marine Laboratory Aberdeen). Cooperation with Dr Aenea Reid (Aberdeen University Computer Centre) in an earlier stage of this work is gratefully acknowledged. Mrs Hanneke Videler-Verheijen was responsible for the painstaking steps between film frames and computer. The Foundation for Fundamental Biological Research (BION), an organization subsidized by the Netherlands Organization for the Advancement of Pure Research (ZWO), financed the cooperation between the authors.

REFERENCES

- AHLBERG, J. H., NILSON, E. N. & WALSH, J. L. (1967). *The Theory of Splines and their Applications*. New York, London: Academic Press.
- BAINBRIDGE, R. (1958). The speed of swimming of fish as related to size and to the frequency and amplitude of tail beat. *J. exp. Biol.* **35**, 109–133.
- BLAXTER, J. H. S. & DICKSON, W. (1959). Observations on swimming speeds of fish. *J. Cons. perm. int. Explor. Mer* **24**, 472–479.
- GRAY, J. (1933). Studies in animal locomotion. I. The movement of fish with special reference to the eel. *J. exp. Biol.* **10**, 88–104.
- GREER WALKER, M. & PULL, G. (1973). Skeletal muscle function and sustained swimming speeds in the coal fish (*Gadus virens* L.). *Comp. Biochem. Physiol.* **44A**, 495–501.
- HESS, F. & VIDELER, J. J. (1984). Fast continuous swimming of saithe (*Pollachius virens*): a dynamic analysis of bending moments and muscle power. *J. exp. Biol.* **109**, 229–251.
- HIMMELBLAU, D. M. (1972). *Applied non-linear Programming*. New York: McGraw.
- LIGHTHILL, M. J. (1960). Note on the swimming of slender fish. *J. Fluid Mech.* **9**, 305–317.
- LIGHTHILL, M. J. (1969). Hydromechanics of aquatic animal propulsion. *Ann. Rev. Fluid Mech.* **44**, 265–301.
- VIDELER, J. J. (1981). Swimming movements, body structure and propulsion in Cod (*Gadus morhua*). In *Vertebrate Locomotion*, (ed. M. H. Day). *Symp. Zool. Soc. Lond.* **48**, 1–27. London: Academic Press.
- VIDELER, J. J. & WARDLE, C. S. (1978). New kinematic data from high speed cine film recordings of swimming Cod (*Gadus morhua*). *Neth. J. Zool.* **28**, 465–484.

- VIDELER, J. J. & WEIHS, D. (1982). Energetic advantages of burst-and-coast swimming of fish at high speeds. *J. exp. Biol.* **97**, 169–178.
- WARDLE, C. S. (1979). Effects of temperature on the maximum swimming speed of fishes. In *Environmental Physiology of Fishes*, (ed. M. A. Ali). *NATO advanced Study Inst. Ser. A.* **35**, 519–531.
- WARDLE, C. S. & VIDELER, J. J. (1980a). Fish swimming. In *Aspects of Animal Movement*, (eds H. T. Elder & E. R. Trueman). *Soc. exp. Biol. Symp.* **5**, 125–150. Cambridge: Cambridge University Press.
- WARDLE, C. S. & VIDELER, J. J. (1980b). How do fish break the speed limit? *Nature, Lond.* **284**, 445–447.
- WEBB, P. W. (1975). Hydrodynamics and energetics of fish propulsion. *Bull. Fish. Res. Bd Can.* **190**, 1–159.